Biosynthesis of Zeaxanthin via Mevalonate in *Paracoccus* Species Strain PTA-3335. A Product-Based Retrobiosynthetic Study†

Wolfgang Eisenreich,*,‡ Adelbert Bacher,‡ Alan Berry,§ Werner Bretzel,§ Markus Hümbelin,§ Rual Lopez-Ulibarri,§ Anne F. Mayer,§ and Alexei Yeliseev§,||

Lehrstuhl für Organische Chemie und Biochemie, Technische Universität München, Lichtenbergstrasse 4, D-85747 Garching, Federal Republic of Germany, and Biotechnology Department, Research and Development, Roche Vitamins AG, CH-4070 Basel, Switzerland

wolfgang.eisenreich@ch.tum.de

Received September 4, 2001

Cultures of the zeaxanthin-producing bacterium *Paracoccus* species strain PTA-3335 (formerly *Flavobacterium*) were grown with supplements of ^{13}C-labeled glucose. Zeaxanthin was isolated and analyzed by ^{13}C NMR spectroscopy. The data showed that the isoprenoid precursors of zeaxanthin were biosynthesized via the mevalonate pathway. The microorganism was found to utilize glucose mainly via the Entner−Doudoroff pathway.

Introduction

Terpenoids constitute one of the largest groups of natural products.[1] They are all biosynthesized from the universal isoprenoid precursors isopentenyl pyrophosphate (IPP) and dimethylallyl pyrophosphate (DMAPP). The biosynthesis of these precursors from acetyl-CoA via mevalonate (reviewed in ref 2) has been studied in considerable detail using animal cells and yeast. A mevalonate-independent second pathway for the biosynthesis of IPP and DMAPP via 1-deoxy-D-xylulose 5-phosphate has been discovered only recently in some eubacteria and plants[3−5;] (reviewed in refs 6−9).

Animals, fungi, and archaea use exclusively the mevalonate pathway. Plants use both isoprenoid pathways for the biosynthesis of different terpenoids. Numerous eubacteria studied to date use the deoxyxylulose pathway, but *Enterococci*, *Streptococci*, and *Staphylococci* appear to use exclusively the mevalonate pathway,[10,11] and *Streptomycetes* have been reported to use both pathways in different phases of their life cycle.[12]

In the mevalonate pathway, the universal terpenoid precursors of IPP and DMAPP are exclusively derived from acetyl-CoA. More specifically, three acetate units afford the five carbon atoms of IPP under loss of one acetate carboxylic group as CO_2 (Figure 1). DMAPP is obtained from IPP by an isomerase.

The non-mevalonate pathway starts with the formation of 1-deoxyxylulose 5-phosphate from pyruvate and glyceraldehyde 3-phosphate catalyzed by 1-deoxyxylulose 5-phosphate synthase.[13,14] The carbohydrate is converted to 2-*C*-methylerythritol 2,4-cyclodiphosphate by a series of four recently discovered reaction steps[15−21] (Figure 1). The steps involved in the conversion of 2-*C*-methylerythritol 2,4-cyclodiphosphate into IPP and DMAPP are as yet unknown. The involvement of an IPP isomerase is not obligatory; rather, it appears that IPP as well as DMAPP can be formed directly from a common precursor.[22,23]

Zeaxanthin (3,3′-dihydroxy-β-carotene) is a yellow carotenoid used commercially in poultry pigmentation

* To whom correspondence should be addressed. Phone: +49-89-289-13043. Fax: +49-89-289-13363. E-mail: wolfgang.eisenreich@ch.tum.de.

† Abbreviations: IPP, isopentenyl diphosphate; DMAPP, dimethylallyl diphosphate; HMG, 3-hydroxy-3-methylglutaryl.

‡ Technische Universität München

§ Roche Vitamins AG.

|| Present address: Kosan Biosciences, Inc., 3832 Bay Center Place, Hayward, CA 94545.

(1) Sacchettini, J. C.; Poulter, C. D. *Science* **1997**, *277*, 1788−1789.

(2) Bochar, D. A.; Friesen, J. A.; Stauffacher, C. V.; Rodwell, V. W. In *Comprehensive Natural Product Chemistry*; Cane, D., Ed.; Pergamon: 1999; Vol. 2, pp 15−44.

(3) Rohmer, M.; Knani, M.; Simonin, P.; Sutter, B.; Sahm, H. *Biochem. J.* **1993**, *295*, 517−524.

(4) Broers, S. J. J. Ph.D. Thesis, ETH Zürich, 1994.

(5) Schwarz, M. K. Ph.D. Thesis, ETH Zürich, 1994.

(6) Eisenreich, W.; Schwarz, M.; Cartayrade, A.; Arigoni, D.; Zenk, M.; Bacher, A. *Chem. Biol.* **1998**, *5*, R221−R233.

(7) Arigoni, A.; Schwarz, M. K. In *Comprehensive Natural Product Chemistry*; Cane, D., Ed.; Pergamon: 1999; Vol. 2, pp 367−399.

(8) Rohmer, M. In *Comprehensive Natural Product Chemistry*; Cane, D., Ed.; Pergamon: 1999; Vol. 2, pp 45−69.

(9) Eisenreich, W.; Rohdich, F.; Bacher, A. *Trends Plant Sci.* **2001**, *6*, 78−84.

(10) Wilding, E. I.; Brown, J. R.; Bryant, A. P.; Chalker, A. F.; Holmes, D. J.; Ingraham, K. A.; Iordanescu, S.; So, C. Y.; Rosenberg, M.; Gwynn, M. N. *J. Bacteriol.* **2000**, *182*, 4319−4327.

(11) Boucher, Y.; Doolittle, W. F. *Mol. Microbiol.* **2000**, *37*, 703−716.

(12) Seto, H.; Watanabe, H.; Furihata, K. *Tetrahedron Lett.* **1996**, *37*, 7979−7982.

(13) Sprenger, G. A.; Schörken, U.; Wiegert, T.; Grolle, S.; deGraaf, A. A.; Taylor, S. V.; Begley, T. P.; Bringer-Meyer, S.; Sahm, H. *Proc. Natl. Acad. Sci. U.S.A.* **1997**, *94*, 12857−12862.

(14) Lois, L. M.; Campos, N.; Putra, S. R.; Danielsen, K.; Rohmer, M.; Boronat, A. *Proc. Natl. Acad. Sci. U.S.A.* **1998**, *95*, 2105−2110.

(15) Takahashi, S.; Kuzuyama, T.; Watanabe, H.; Seto, H. *Proc. Natl. Acad. Sci. U.S.A.* **1998**, *95*, 9879−9884.

(16) Rohdich, F.; Wungsintaweekul, J.; Fellermeier, M.; Sagner, S.; Herz, S.; Kis, K.; Eisenreich, W.; Bacher, A.; Zenk, M. H. *Proc. Natl. Acad. Sci. U.S.A.* **1999**, *96*, 11758−11763.

(17) Kuzuyama, T.; Takagi, M.; Kaneda, K.; Dairi, T.; Seto, H. *Tetrahedron Lett.* **2000**, *41*, 703−706.

(18) Lüttgen, H.; Rohdich, F.; Herz, S.; Wungsintaweekul, J.; Hecht, S.; Schuhr, C. A.; Fellermeier, M.; Sagner, S.; Zenk, M. H.; Bacher, A.; Eisenreich, W. *Proc. Natl. Acad. Sci. U.S.A.* **2000**, *97*, 1062−1067.

(19) Kuzuyama, T.; Takagi, M.; Kaneda, K.; Watanabe, H.; Dairi, T.; Seto, H. *Tetrahedron Lett.* **2000**, *41*, 2925−2928.

(20) Herz, S.; Wungsintaweekul, J.; Schuhr, C. A.; Hecht, S.; Lüttgen, H.; Sagner, S.; Fellermeier, M.; Eisenreich, W.; Zenk, M. H.; Bacher, A.; Rohdich, F. *Proc. Natl. Acad. Sci. U.S.A.* **2000**, *97*, 2486-2490.

(21) Takagi, M.; Kuzuyama, T.; Kaneda, K.; Watanabe, H.; Dairi, T.; Seto, H. *Tetrahedron Lett.* **2000**, *41*, 3395−3398.

(22) Giner, J.-L.; Jaun, B.; Arigoni, D. *J. Chem. Soc., Chem. Commun.* **1998**, 1857−1858.

(23) Rodriguez-Concepcion, M.; Campos, N.; Lois, L. M.; Maldonado, C.; Hoeffler, J.-F.; Grosdemange-Billiard, C.; Rohmer, M.; Boronat, A. *FEBS Lett.* **2000**, *473*, 328−332.

10.1021/jo016084r CCC: $22.00
Published on Web 01/05/2002

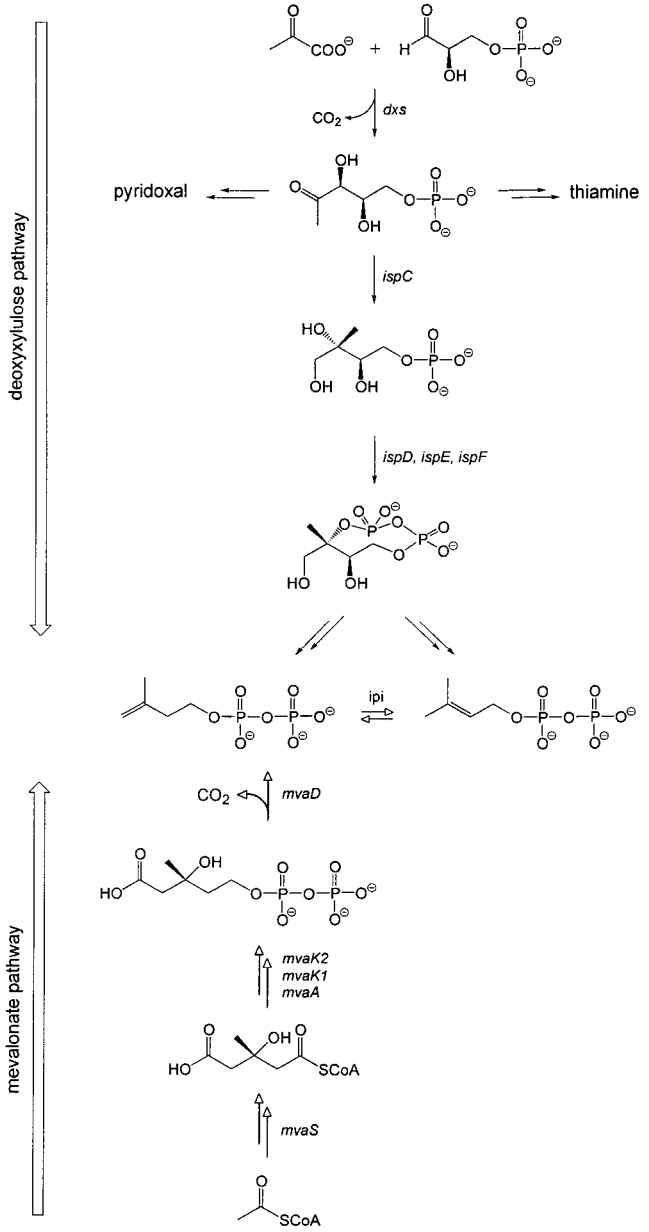

Figure 1. Pathways of isoprenoid biosynthesis: *Dxs*, 1-deoxy-D-xylulose 5-phosphate synthase; *ispC*, 2-*C*-methyl-D-erythritol 4-phosphate synthase; *ispD*, 4-diphosphocytidyl-2-*C*-methyl-D-erythritol synthase; *ispE*, 4-diphosphocytidyl-2-*C*-methyl-D-erythritol kinase; *ispF*, 2-*C*-methyl-D-erythritol 2,4-cyclodiphosphate synthase; *ipi*, isopentenyl diphosphate isomerase; *mvaK2*, phosphomevalonate kinase; *mvaD*, mevalonate diphosphate decarboxylase; *mvaK1*, mevalonate kinase; *mvaA*, HMG-CoA reductase; *mvaS*, HMG-CoA synthase.

and in human nutrition. In poultry, zeaxanthin, together with lutein, contributes to the coloration of egg yolk and skin,[24] while in humans there is evidence that a diet rich in these carotenoids decreases the risk of age-related macular degeneration.[25] While zeaxanthin can be obtained from natural sources and produced by chemical synthesis, a fermentation process for zeaxanthin production is a commercially interesting prospect. In the present paper, we describe one aspect of our effort to apply metabolic engineering to improve zeaxanthin production in the bacterium *Paracoccus* sp. strain PTA-3335, namely, the determination of metabolic flux to the zeaxanthin precursors IPP and DMAPP. *Paracoccus* sp. strain PTA-3335 is a mutant derived from a zeaxanthin-producing marine bacterium originally classified as a species of *Flavobacterium*.[26] Goodwin[27] showed that cell-free extracts of a strain related to PTA-3335 converted labeled mevalonate into zeaxanthin, proving the existence of the mevalonate pathway for IPP and DMAPP production. However, the latter work was done prior to the discovery of the non-mevalonate pathway, and, accordingly, did not consider possible metabolic flux contributions via alternative pathways. As mentioned above, some bacteria possess both pathways of IPP biosynthesis, and a quantitative assessment of metabolic flux inside the metabolic network is required to yield reliable conclusions. By retrobiosynthetic analysis we now confirm that zeaxanthin biosynthesis occurs exclusively via the mevalonate pathway in *Paracoccus* sp. strain PTA-3335, and further show that this organism metabolizes glucose mainly through the Entner−Doudoroff pathway.

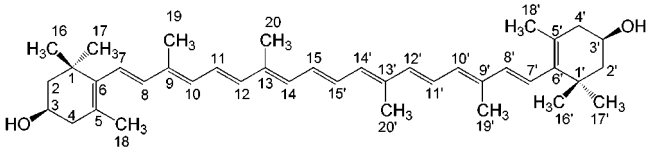

Figure 2. Structure of zeaxanthin.

Results and Discussion

To determine the biosynthetic origin of isoprenoid precursors in *Paracoccus* sp. strain PTA-3335, we cultured the bacterium with supplements of [1-$^{13}C_1$]-, [2-$^{13}C_1$]-, [6-$^{13}C_1$]-, or [U-$^{13}C_6$]glucose. Each labeled glucose was proffered together with an excess of unlabeled glucose (see the Experimental Section).

Zeaxanthin (Figure 2) was isolated from the cultures and was analyzed by ^{13}C NMR spectrometry. The carotenoid comprises a total of 40 carbon atoms with eight isoprenoid moieties (2 DMAPP and 6 IPP units); only 20 ^{13}C NMR signals are observed due to the C_2 symmetry of zeaxanthin.

The ^{13}C abundance for all nonequivalent carbon atoms was determined by comparison of ^{13}C NMR signal intensities with those in spectra of unlabeled zeaxanthin and by evaluation of the ^{1}H^{13}C coupling satellites in ^{1}H NMR spectra (Table 1). The fraction of jointly transferred carbon atom pairs in the experiment with [U-$^{13}C_6$]glucose was determined by integration of the coupling satellites (Table 1).

In the experiment with the mixture of [U-$^{13}C_6$]glucose and unlabeled glucose, all carbon atoms of zeaxanthin were labeled and showed satellites due to ^{13}C^{13}C couplings (Table 1). Figure 3 shows the signals representing the zeaxanthin atoms derived from the DMAPP starter unit. The signals of four carbon atoms (C-1, C-2, C-3, and C-16) had intense satellites due to ^{13}C^{13}C couplings (61.2% ± 0.6% in the global NMR signal intensity of a

(24) Hadden, W. L.; Watkins, R. H.; Levy, L. W.; Regalado, E.; Rivadeneira, D. M.; van Breemen, R. B.; Schwartz, S. J. *J. Agric. Food Chem.* **1999**, *47*, 4189−4194.

(25) Seddon, J. M.; Ajani, U. A.; Sperduto, R. D.; Hiller, R.; Blair, N.; Burton, T. C.; Farber, M. D.; Gragoudas, E. S.; Haller, J.; Miller, D. T.; Yannuzzi, L. A.; Willett, W. *JAMA, J. Am. Med. Assoc.* **1994**, *272*, 1413−1420.

(26) Schocher, A. J.; Wiss, O. U.S. Patent 3,891,504, 1975.

(27) Goodwin, T. W. *Biochem. Soc. Symp.* **1972**, *35*, 233−244.

Table 1. NMR Data of Zeaxanthin from *Paracoccus* sp. Strain PTA-3335 Supplied with ^{13}C-Labeled Glucoses

			^{13}C abundance of zeaxanthin from the experiment with labeled glucose				
position	$\delta(^{13}C)^a$ (ppm)	$J_{CC}{}^b$ (Hz)	[1-$^{13}C_1$]glucose (% ^{13}C)	[2-$^{13}C_1$]glucose (% ^{13}C)	[6-$^{13}C_1$]glucose (% ^{13}C)	[U-$^{13}C_6$] glucose (% ^{13}C)	% $^{13}C^{13}C$
1, 1′	37.13	36.0 (16, 16′)	1.10	10.71	2.22	3.47	61.2
2, 2′	48.46	35.8 (3, 3′)	1.20	2.58	10.27	3.65	61.1
3, 3′	65.10	35.8 (2, 2′)	1.12	12.47	2.38	3.64	60.4
4, 4′	42.57	37.1	1.27	2.59	10.63	3.89	8.4
5, 5′	126.17	44.2 (18, 18′)	1.14	12.45	3.19	3.68	61.1
6, 6′	137.77	56.4 (7, 7′)	1.30	2.15	9.98	3.60	60.4
7, 7′	125.59	56.2 (6, 6′)	1.12	10.11	2.82	4.09	61.4
8, 8′	138.50	71.6, 55.7	1.28	2.24	9.95	3.92	4.3, 5.0
9, 9′	135.69	43.1 (19, 19′)	1.12	9.53	2.95	3.84	61.7
10, 10′	131.31	59.7 (11, 11′)	1.21	3.18	9.61	3.80	61.1
11, 11′	124.93	59.7 (10, 10′)	1.10	8.79	2.70	4.02	61.0
12, 12′	137.57	70.5	1.20	2.01	8.80	3.59	5.1
13, 13′	136.48	43.1 (20, 20′)	1.12	9.86	3.59	3.93	61.4
14, 14′	132.60	60.4 (15, 15′)	1.21	2.83	10.51	3.77	59.5
15, 15′	130.08	60.4 (14, 14′)	1.12	9.18	3.33	4.02	61.2
16, 16′	30.26	36.3 (1, 1′)	1.27	3.19	12.31	3.91	62.0
17, 17′	28.73	34.9 (1, 1′)	1.30	3.43	12.31	3.88	6.0
18, 18′	21.62	44.2 (5, 5′)	1.27	3.01	11.66	3.70	62.0
19, 19′	12.82	43.1 (9, 9′)	1.29	3.12	11.64	3.86	62.3
20, 20′	12.75	42.9 (13, 13′)	1.33	3.21	11.99	3.75	62.1

[a] Referenced to the solvent signal. [b] From the spectrum of zeaxanthin obtained from the experiment with [U-$^{13}C_6$]glucose. Coupling partners are given in parentheses.

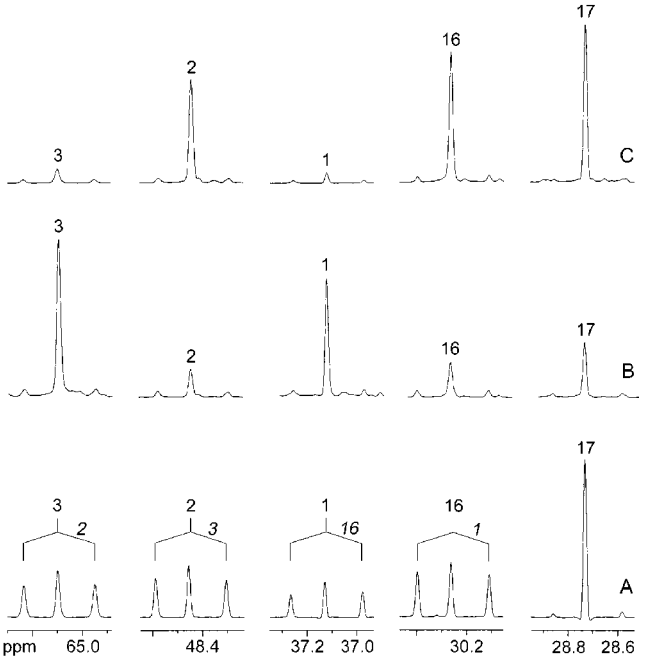

Figure 3. ^{13}C NMR signals of biosynthetic zeaxanthin samples from *Paracoccus* sp. strain PTA-3335: (A) from [U-$^{13}C_6$]glucose, (B) from [2-$^{13}C_1$]glucose, and (C) from [6-$^{13}C_1$]-glucose.

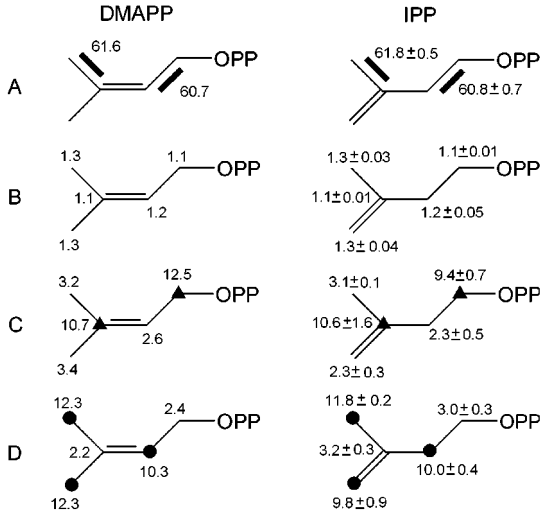

Figure 4. Reconstructed labeling patterns of isoprenoid precursor units of zeaxanthin: (A) from [U-$^{13}C_6$]glucose, (B) from [1-$^{13}C_1$]glucose, (C) from [2-$^{13}C_1$]glucose, and (D) from [6-$^{13}C_1$]glucose. ▲ and ● indicate atoms enriched from [2-$^{13}C_1$]- and [6-$^{13}C_1$]glucose, respectively. Bars indicate contiguous ^{13}C pairs from [U-$^{13}C_6$]glucose. Numbers indicate ^{13}C abundances (B−D) or relative fractions of multiply ^{13}C labeled isotopomers (A).

given atom; the central signals represent material derived from unlabeled glucose; Table 1). The signal accounting for the methyl atoms C-17/C-17′ displayed only weak ^{13}C-coupled satellites at a relative intensity of 6%. None of the signals showed evidence of long-range coupling. Carbon connectivity was easily gleaned from $^{13}C^{13}C$ coupling constants (Table 1) and from two-dimensional INADEQUATE experiments.

Three carbon atoms of the DMAPP unit (C-2, C-16, and C-17) acquired label from [6-$^{13}C_1$]glucose (Figure 3C), and two carbons (C-1 and C-3) were labeled from [2-$^{13}C_1$]-glucose (Figure 3B). No significant amounts of label were contributed to zeaxanthin by [1-$^{13}C_1$]glucose (Table 1). The labeling signatures of the DMAPP unit are summarized in Figure 4.

The labeling patterns of the IPP building block could be reconstructed accurately as shown by the standard deviations obtained by averaging over three IPP-derived motifs (Figure 4). The reconstructed labeling patterns of IPP and DMAPP were identical within the experimental limits. As a result, C-1 and C-3 of IPP/DMAPP acquired label from [2-$^{13}C_1$]glucose, whereas C-2, C-4, and C-5 of IPP/DMAPP were ^{13}C-enriched from [6-$^{13}C_1$]glucose. [1-$^{13}C_1$]Glucose appeared to transfer label to C-2, C-4, and C-5 of DMAPP/IPP at levels close to above the detection limit.

Glucose metabolism in eubacteria occurs mainly via the glycolytic pathway (also used by eukaryotes) or the Entner−Doudoroff pathway. Glycolysis generates two triose phosphate molecules from glucose. The fate of labeled glucose carbon atoms during glycolysis is shown

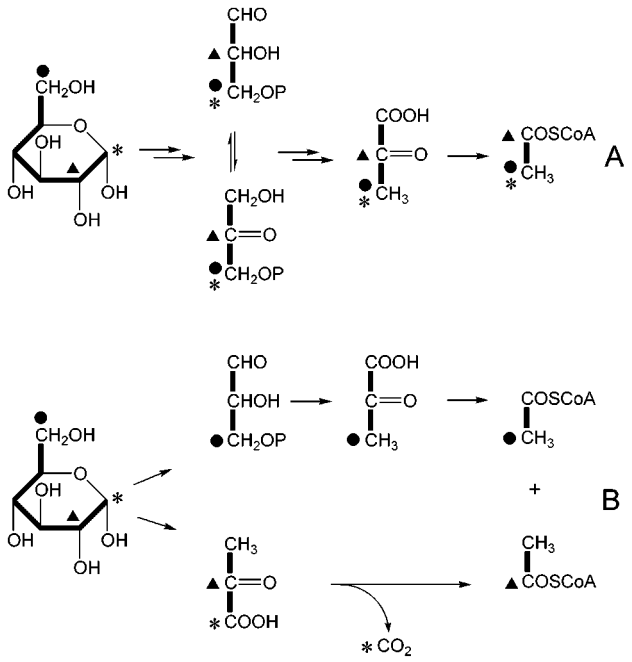

Figure 5. Prediction of labeling patterns via different metabolic pathways: (A) glycolysis, (B) Entner−Doudoroff pathway. *, ▲, and ● indicate atoms enriched from [1-$^{13}C_1$]-, [2-$^{13}C_1$]-, and [6-$^{13}C_1$]glucose, respectively. Bars indicate contiguous ^{13}C atoms from [U-$^{13}C_6$]glucose.

in Figure 5A. C-1 and C-6 of glucose are both diverted to the 3-position of the triose phosphate produced.

The Entner−Doudoroff pathway, on the other hand, converts glucose to a mixture of glyceraldehyde 3-phosphate and pyruvate. Notably, label from C-1 of glucose is exclusively diverted to C-1 of pyruvate, and label from C-6 of glucose is exclusively diverted to C-3 of glyceraldehyde 3-phosphate (Figure 5B).

The products of both glucose catabolic pathways can serve as starting material for both isoprenoid pathways as summarized in Figure 5. Pyruvate as well as triose phosphate can be converted to acetyl-CoA, the precursor of the mevalonate pathway. Transformation of pyruvate obtained via the Entner−Doudoroff pathway to acetyl-CoA is accompanied by the loss of C-1 from glucose. On the other hand, glucose catabolism via the glycolytic pathway should divert label from C-1 as well as C-6 of glucose to the methyl group of acetyl-CoA.

Figure 6 predicts the labeling patterns of IPP by all four combinations of the two terpenoid pathways and the two glucose catabolic pathways. It is obvious that the labeling strategies used in the experiments described above should result in highly characteristic labeling patterns for each specific case.

The experimental labeling patterns determined above were compared with the various predictions. The experimentally observed enrichment and $^{13}C^{13}C$ coupling patterns (Figure 4) were in perfect agreement with the labeling pattern required for the combination of the Entner−Doudoroff pathway and the mevalonate pathway (Figure 6B). The low level of incorporation from [1-$^{13}C_1$]-glucose into C-2, C-4, and C-5 of DMAPP/IPP could indicate low metabolic flux via glycolysis (cf. Figure 6A).

The mevalonate pathway can at best contribute blocks of two carbon atoms to terpenoids. On the other hand, three carbon atoms can be jointly delivered to isoprenoids via [U-$^{13}C_3$]triose phosphate precursors via the non-mevalonate pathway. Although such three-carbon blocks become separated by the rearrangement involved in the deoxyxylulose pathway, blocks of three labeled carbon atoms can still be recognized via long-range coupling, which has been in fact observed in lutein biosynthesized from [2,3,4,5-$^{13}C_4$]-1-deoxy-D-xylulose by cultured plant cells.[28] No such long-range coupling occurred in the present experiments with *Paracoccus* sp. strain PTA-3335.

It should be noted that the predictive approach used for data analysis permits the unequivocal assessment of glucose catabolism from the analysis of a single downstream natural product formed in the culture.

The experimental data also yielded information on the stereochemical aspects of the formation of the cyclohexane ring of zeaxanthin. The diasterotopic methyl groups C-16 and C-17 of zeaxanthin give rise to nonisochronous signals. The stereospecific assignments of zeaxanthin NMR signals have been reported previously by Britton et al.[29]

The zeaxanthin methyl group C-16 resonating at 30.26 ppm showed coupling to C-1. Hence, it is biosynthetically equivalent to the (*Z*)-methyl group of DMAPP. Protonation of the linear precursor in the indicated chair conformation yields a cyclic cation in which H−x is located in an axial position (Figure 7). Subsequent elimination of H−x^+ affords the double bond between C-5 and C-6 and the correct stereochemical arrangement of the two biogenetically nonequivalent methyl groups at C-1. The results are in line with the stereochemical course of ring formation in certain plants and bacteria.[28,30,31]

Experimental Section

Materials. Unlabeled D-glucose monohydrate was purchased from Fluka (Milwaukee, WI). [U-$^{13}C_6$]-D-Glucose was purchased from Isotec (Miamisburg, OH). [1-$^{13}C_1$]-D-glucose, [2-$^{13}C_1$]-D-glucose, and [6-$^{13}C_1$]-D-glucose were from Cambridge Isotope Laboratories (Andover, MA). Yeast extract and peptone (from casein, pancreatically digested) were purchased from EM Science (Gibbstown, NJ). All other salts and solvents were analytical grade and were purchased from standard chemical suppliers.

Strain and Culture Conditions. *Paracoccus* sp. strain PTA-3335 is a descendent of *Paracoccus* sp. strain R-1512 (ATCC 21588). These zeaxanthin-producing bacteria were formerly classified as *Flavobacterium* sp. (A. Berry et al., manuscript in preparation).

Cultures for labeling experiments were grown in Bioflo 3000 bioreactors (New Brunswick Scientific, Edison, NJ) in a medium containing, per liter, 30 g of total D-glucose (see below for ratios of ^{13}C-labeled to unlabeled glucose), 20 g of yeast extract, 10 g of peptone, 10 g of NaCl, 5 g of $MgSO_4 \cdot 7H_2O$, 1.5 g of $(NH_4)_2HPO_4$, 1.25 g of K_2HPO_4, 0.4 g of $(NH_4)_2Fe(SO_4)_2 \cdot 6H_2O$, 375 mg of $CaCl_2 \cdot 2H_2O$, 30 mg of $ZnSO_4 \cdot 7H_2O$, 25 mg of $FeCl_3 \cdot 6H_2O$, 10 mg of $MnSO_4 \cdot H_2O$, 1 mg of $NiSO_4 \cdot 6H_2O$, 30 mg of NaEDTA, and 18.75 μL of 37% hydrochloric acid. The amounts of each ^{13}C-labeled glucose used (expressed as a percentage of the total glucose (30 g/L) in the medium) in four separate experiments were (condition 1) 4% [U-$^{13}C_6$]-D-glucose, (condition 2) 50% [1-$^{13}C_1$]-D-glucose, (condition 3) 25% [2-$^{13}C_1$]-D-glucose + 1% [U-$^{13}C_6$]-D-glucose, and (condition 4) 25%

(28) Arigoni, D.; Sagner, S.; Latzel, C.; Eisenreich, W.; Bacher, A.; Zenk, M. H. *Proc. Natl. Sci. U.S.A.* **1997**, *94*, 10600−10605.
(29) Britton, G.; Goodwin, T. W.; Lockley, W. J. S.; Mundy, A. P.; Patel, N. J. *J. Chem. Soc., Chem. Commun.* **1979**, 27−28.
(30) Mohanty, S. S.; Uebelhart, P.; Eugster, C. H. *Helv. Chim. Acta* **2000**, *83*, 2036−2052.
(31) Kakinuma, K.; Dekishima, Y.; Matsushima, Y.; Eguchi, T.; Misawa, N.; Takagi, M.; Kuzuyama, T.; Seto, H. *J. Am. Chem. Soc.* **2001**, *123*, 1238−1239.

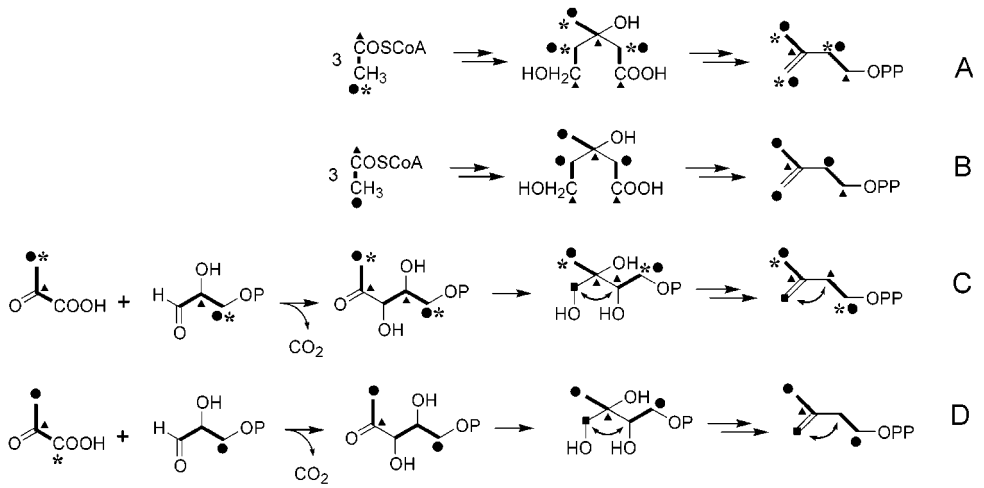

Figure 6. Prediction of labeling patterns of IPP formed via different metabolic pathways: (A) glycolysis and mevalonate pathways, (B) Entner−Doudoroff and mevalonate pathways, (C) glycolysis and deoxyxylulose pathways, (D) Entner−Doudoroff and deoxyxylulose pathways. For details, see the caption to Figure 5.

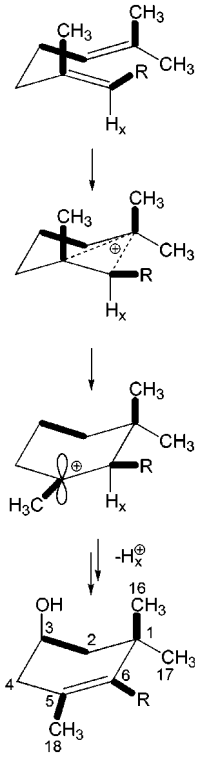

Figure 7. Stereochemical course of ring formation during the biosynthesis of zeaxanthin in *Paracoccus* sp. strain PTA-3335. Bars indicate contiguous ^{13}C atoms from [U-$^{13}C_6$]glucose.

[6-$^{13}C_1$]-D-glucose + 1% [U-$^{13}C_6$]-D-glucose. A control with only unlabeled glucose was also included. The cultures were grown for 22−24 h, at which time no glucose was left in the medium. Cultivation conditions were 28 °C, pH 7.2 (controlled with 25% H_3PO_4 and 28% NH_4OH), dissolved oxygen controlled (in a cascade with agitation) at a minimum of 40%, agitation rate and aeration rate 300 rpm (minimum) and 1 vvm, respectively.

Isolation of Zeaxanthin. Cultures were cooled to 15 °C. Ethanol (500 mL/L of culture) was added. The mixture was stirred at 100 rpm for 20 min and centrifuged for 20 min at 5000*g*. The supernatant was discarded. The wet pellet was extracted with 5 volumes of tetrahydrofuran (THF) for 20 min with stirring. The extracted mixture was centrifuged, and the resulting pellet extracted a second time with 1 volume of THF. The supernatants (extracts) were combined and concentrated to 50 mL under reduced pressure, and 5 mL of hexane was added. After mixing, the system formed an emulsion which could be separated by centrifugation. The aqueous phase was collected, diluted with an equal volume of saturated NaCl solution, and re-extracted with dichloromethane. The dichloromethane phase was collected and combined with the THF/hexane phase. The mixture of organic extracts was concentrated again in a rotary evaporator to remove dichloromethane. The solution was then applied to a silica gel column which was developed with a mixture of *n*-hexane and ether (1:1). About 2 L of solvent was needed to elute the main band containing zeaxanthin. This fraction was evaporated to dryness under reduced pressure. The residue was dissolved in a small amount of dichloromethane at 40 °C, and the solution was then allowed to cool slowly. Hexane was added to the mixture dropwise until turbidity was observed. The crystallization was complete within 48 h at 4 °C. The crystals were collected on a paper filter, washed with cold methanol, and dried under vacuum.

NMR Spectroscopy. ^1H NMR and ^{13}C NMR spectra were recorded at 500.13 and 125.6 MHz, respectively, with a Bruker DRX 500 spectrometer. Data were acquired and processed with standard Bruker software (XWINNMR). The solvent was deuterated chloroform.

Determination of ^{13}C-Labeling Patterns. The methods used for determining ^{13}C enrichment have been described in detail previously.[32] Briefly, ^{13}C NMR spectra of the isotope-labeled zeaxanthin samples and of a zeaxanthin sample at natural ^{13}C abundance were recorded under the same experimental conditions. Integrals were determined for every ^{13}C NMR signal, and the signal integral for each respective carbon atom in the labeled compound was referenced to that of the natural abundance material, thus affording relative ^{13}C abundances for each position in the labeled molecular species. The relative abundances were then converted into absolute abundances (% ^{13}C in Table 1) from $^1H^{13}C$ coupling satellites in the ^1H NMR signal of H-18 at 1.71 ppm.

In the ^{13}C NMR spectrum of a multiply labeled zeaxanthin sample (from the experiment with [U-$^{13}C_6$]glucose), each satellite was integrated separately. The integral of each respective satellite pair was then referenced to the total signal integral of a given carbon atom (% $^{13}C^{13}C$ in Table 1).

Acknowledgment. We thank Angelika Werner and Fritz Wendling for expert help with the preparation of the manuscript, and Dr. Markus Goese for helpful discussions.

JO016084R

(32) Eisenreich, W.; Bacher, A. In *Genetic Engineering. Principles and Methods;* Setlow, J. K., Ed.; Kluwer Academic/Plenum Publishers: New York, 2000; Vol. 22, pp 121−153.